Stroke

CLINICAL AND POPULATION SCIENCES

Brain Peri-Hematomal Area, a Strategic Interface for Blood Clearance: A Human Neuropathological and Transcriptomic Study

Laurent Puy, MD, PhD; Romain Perbet, MD, PhD; Martin Figeac, MD, PhD; Bélinda Duchêne; Vincent Deramecourt, MD, PhD; Charlotte Cordonnier, MD, PhD; Vincent Bérézowski, PhD

BACKGROUND: Enhancing the blood clearance process is a promising therapeutic strategy for intracerebral hemorrhage (ICH). We aimed to investigate the kinetic of this process after ICH in human brain tissue through the monocyte-macrophage scavenger receptor (CD163)/HO-1 (hemoxygenase-1) pathway.

METHODS: We led a cross-sectional post-mortem study including 22 consecutive ICH cases (2005–2019) from the Lille Neurobank. Cases were grouped according to the time of death: ≤72 hours, 4 to 7 days, 8 to 15 days, 16 to 90 days, and >90 days after ICH onset. Paraffin-embedded tissue was extracted from 4 strategic areas, including hematoma core and peri-hematomal area to perform histological investigations. Additionally, we extracted RNA from the peri-hematomal area of 6 cases to perform transcriptomic analysis.

RESULTS: We included 19 ICH cases (median age: 79 [71–89] years; median delay ICH-death: 13 [5–41] days). The peri-hematomal area concentrated most of reactive microglia, CD163/HO-1 and iron deposits as compared with other brain areas. We found a surge in the blood clearance process from day 8 to day 15 after ICH onset. Transcriptomic analysis showed that HO-1 was the most upregulated gene (2.81±0.39, adjusted $P=1.11\times10^{-10}$) and CD163 the sixth (1.49±0.29, adjusted $P=1.68\times10^{-5}$). We also identified several upregulated genes that exert a beneficial role in terminating inflammation and enhancing tissue repair.

CONCLUSIONS: We provide histological and transcriptomic-based evidence in humans for the key role of peri-hematomal area in endogenous blood clearance process through the CD163/HO-1 pathway, especially from day 8 after ICH and favored by an anti-inflammatory environment. Our findings contribute to identify innovative therapeutic strategies for ICH.

GRAPHIC ABSTRACT: A graphic abstract is available for this article.

Key Words: cerebral hemorrhage ■ edema ■ hemoglobin ■ inflammation ■ macrophage ■ neuropathology

Spontaneous intracerebral hemorrhage (ICH) is a devastating cause of mortality and morbidity devoid of specific treatment.[1] To develop efficient therapeutic strategies for ICH, a deep understanding of its pathophysiology is warranted. The pathological process of ICH includes the primary brain damage resulting from immediate mass effect owing to hematoma formation, and the delayed secondary brain injury occurring in the peri-hematomal area (PHA). In the ensuing days after ICH, lysis of erythrocytes leads to the release of free hemoglobin, a major component of secondary damage.[2] Therefore, the expected benefit of blood evacuation is potentially high. Two therapeutic options to achieve this goal are currently under investigation: a mechanical strategy with minimally invasive surgery,[3] and a pharmacological one, aiming at enhancing the endogenous

Correspondence to: Charlotte Cordonnier, MD, PhD, Neurology & stroke unit, Univ. Lille, INSERM U 1171, CHU LILLE, Hopital Salengro, BD Emaile Laine, Lille 59000, France. Email charlotte.cordonnier@univ-lille.fr
This article was sent to Hanne Christensen, Senior Guest Editor, for review by expert referees, editorial decision, and final disposition.
Supplemental Material is available at https://www.ahajournals.org/doi/suppl/10.1161/STROKEAHA.121.037751.
For Sources of Funding and Disclosures, see page 2034.

Stroke is available at www.ahajournals.org/journal/str

Nonstandard Abbreviations and Acronyms

CD163	monocyte-macrophage scavenger receptor
GAT-1	γ-aminobutyric acid transporter 1
HO-1	hemeoxygenase-1
Iba1	ionized calcium-binding adapter molecule 1
ICH	intracerebral hemorrhage
ISBT	ipsilateral surrounding brain tissue
PHA	peri-hematomal area

clearance of blood.[4,5] The second is of particular interest but requires a better understanding of the blood clearance process that occurs spontaneously in the brain of patients with ICH.

See related article, p 2036

One of the primary natural mechanisms protecting the tissue against the deleterious effects of free hemoglobin is ruled by CD163 (monocyte-macrophage scavenger receptor), a monocyte-macrophage scavenger receptor expressed by many cells harboring a phagocytic function such as activated microglia or recruited macrophages.[6] CD163 acts as an endocytic receptor for hemoglobin–haptoglobin complexes and is, therefore, involved in sequestering toxic hemolysis products.[7,8] After its incorporation, hemoglobin is broken down into Fe^{2+}, carbon monoxyde, and biliverdin via catalysis driven by HO-1 (hemeoxygenase-1).[9] HO-1 has also antioxydant, anti-inflammatory, and antiapoptotic properties.[10] Therefore, the CD163/HO-1 pathway represents a basic line of defense against hemoglobin neurotoxicity by facilitating its clearance.[11] Although its contribution to hematoma clearance is well-established in experimental studies,[12–14] few human data are available.[15–18] In the current study, we investigated spatial and temporal expression of CD163/HO-1 pathway in human brain tissue from patients deceased from ICH. To do so, we performed both histological and transcriptomic analyses. The latter approach additionally brought a novel insight into a broader spectrum of mechanisms that mediate secondary injury and repair after ICH.

METHODS

Standard Protocol Approvals, Registration, and Patient Consents

Human brains were obtained from the Lille Neurobank (CRB/CIC1403 Biobank, BB-0033-00030, agreement DC-2008-642), which fulfils the criteria of the local laws and regulations on biological resources with donor consent, data protection, and ethical committee review. This study adheres to the STROBE cross-sectional study guidelines. All data relevant to the study are included in the article or uploaded as Supplemental Material. Other data are available upon reasonable request.

Human Brain Sampling

We included 22 consecutive cases (2005–2019) from the Lille Neurobank (France) of patients with ICH who came to autopsy.[19] All autopsies were performed 12 to 36 hours after death. Postmortem examination and brain sampling methods are reported elsewhere.[20] ICH volume was manually segmented using Mango software on the first brain imaging performed (brain magnetic resonance imaging [MRI] or computed tomography [CT] scan) at admission. To assess the potential spreading of CD163 and HO-1 expressions within ICH core and surrounding tissue, paraffin-embedded tissue blocks were analyzed from 4 distinct areas: (1) within the hematoma, (2) within the PHA, (3) next to the PHA within ipsilateral surrounding brain tissue (ISBT). Lastly, a fourth control contralateral area was analyzed.

Staining and Immunohistochemistry

Sections of formalin-fixed paraffin embedded tissue were stained with hematoxylin–eosin for a global structural analysis of the tissues. We used Iba1 (ionized calcium-binding adapter molecule 1), CD163 and HO-1 immunolabellings to assess microglial activation, scavenging, and hemoglobin degradation activities. As a result of hematoma clearance, we used a Perl's staining to quantify iron accumulation. All stainings and immunolabellings were performed on serial-sections of 5 µm each with an automated method (see Supplemental Material). A brightfield slide scanner (Zeiss Axioscan Z1) digitized the whole tissue section at 20-fold magnification after staining. Immunolabelled sections were independently analyzed by 2 experienced operators (Drs Puy and Bérézowski). A staining surface ratio ([stacking surface/whole section surface]) was calculated with a semi-automated method using ImageJ software to quantify the positively stained or labeled surface in each area.

Nanostring and Gene Identification

Sample Preparation and RNA Extraction

Formalin-fixed paraffin embedded tissue samples were collected from 6 patients for RNA extraction. These 6 patients died between day 6 and day 17 after ICH. Two experienced investigators (Drs Puy and Perbet) examined the specimen on hematoxylin–eosin-stained slides and annotated a 0.25 cm^2 area of interest. The tissue of the area of interest was then scraped off on serial slides. For each patient, peri-hematoma tissue and a reference contralateral tissue of the same Brodmann area were selected. RNA was prepared according to the manufacturer's instructions using the Qiagen RNeasy Micro RNA kit (Catalog No. 74004; Qiagen, Courtaboeuf, France). The purified RNA was eluted in RNase-free water. Quantitation was performed using the NanoDrop 2000c (Thermo Fisher Scientific, Waltham, MA). Quality of RNA was assessed with a bioanalyzer 2100 (Agilent Technologies, Santa Clara, CA).

Gene Expression Profiling

NanoString nCounter RNA expression profiling was performed according to the manufacturer's instructions with 261 to 526 ng RNA input to adapt to the quality of RNA and using the nCounter Neuroinflammation Panel (NanoString, Seattle, WA) on 6 relevant cases. The list of the 770 genes screened is available in the Table S2. Output reporter code counts file and quality control was performed using nSolver Analysis Software (version 4.0; NanoString, Seattle, WA) to generate raw counts data. Further analysis including normalization and differential expression were done with R (https://www.R-project.org) and DESeq2 package.[21] Normalization was performed using the 13 housekeeping genes included in the commercial design. Differentially expressed gene was defined by the association of an adjusted *P* value (Benjamini and Hochberg method) $<6\times10^{-4}$ (ie, $P<1\times10^{-5}$) and log 2-fold change >1 or <−1.

Statistical Analysis

Continuous, ordinal, and categorical variables were expressed as the mean±SEM, the median (interquartile range) or the number (percentage), respectively. We first compared the expression levels of Iba1, CD163, and HO-1 between areas of interest (hematoma core, PHA, ISBT versus contralateral area as reference). We then compared expression levels between different time-points. To do so, ICH cases were grouped according to the time of death: ≤72 hours (n=2), from day 4 to day 7 (n=4), from day 8 to day 15 (n=5), from day 16 to day 90 (n=4), and >90 days (n=4). We used a Kruskal-Wallis with Tukey post hoc test to compare the different area of interests and timepoints. GraphPad Prism software was used to perform the statistical analysis, with the *P* value considered as significant when <0.05.

RESULTS

Study Population

Between 2005 and 2019, 22 patients with ICH came to autopsy. Among them, 3 ICH were due to an underlying vascular malformation (arteriovenous malformation, n=2 and cavernous malformation, n=1). Therefore, we included 19 spontaneous ICH cases in this study (median age: 79 [71–89] years, 8 men). Median delay between ICH onset and death was 13 days (5–41). Median ICH volume was 84 (46–111). None of the included patients had undergone a neurosurgical intervention. Characteristics of each case are reported in Table S1.

Spatial Distribution of IBA1, CD163, and HO-1 Expression

On visual examination of Iba1 immunolabelled sections, microglia was observed in all cases (n=19/19). Iba1 was mainly expressed within the PHA (Figure 1A), and to a lesser extent in the ISBT (0.07±0.007 and 0.04±0.004, respectively; *P*<0.0001 and 0.028 versus control area). Ramified (resting) microglial cells were seen in locations distant from the hematoma while amoeboid (reactive) microglia cells were observed from 24-hour post-ICH at the hematoma border.

The CD163 expression level was maximal within the PHA (0.12±0.02, *P*<0.0001 versus control area) but also significantly observed in ISBT (0.05±0.01, *P*=0.042 versus control area; Figure 1B). In these areas, CD163 positive cells were observed at the border of the ICH core and in perivascular spaces of small vessels within the PHA. There was a trend towards increased CD163 expression in the hematoma core (*P*=0.07 versus control area).

HO-1 expression was exclusively and differentially increased within the PHA (0.016±0.004, *P*=0.002 versus control area; Figure 1C).

Iron deposits were mostly observed within PHA (0.014±0.003, *P*=0.0006 versus control area), and in a lesser extent, in the hematoma core (0.005±0.001, *P*=0.02 versus control area; Figure 1D).

Temporal Distribution of Reactive Microglia, CD163/HO-1 Expression and Iron Deposition Within the PHA

Iba1 positive cells were observed in the PHA in the early 72 hours (0.038 [0.030–0.056]) with both ramified and ameboid profile. The Iba1 expression increased from day 4 (0.054 [0.028–0.086]) and peaked from day 8 to 15 (0.11 [0.07–0.15]; *P*=0.028 with T1 as reference) with an exclusively ameboid profile. From day 16, we observed a slight decrease (0.07 [0.06–0.11]). From 90 days, there was still a substantial expression of Iba1 (0.045 [0.037–0.062]; *P*=0.019 with control area as reference; Figure 1A).

We found CD163 positive cells in the early 72 hours (0.021 [0.014–0.028]) but the increase in the expression level was exponential from day 8 onwards (0.15 [0.13–0.21]). CD163 expression level reached a peak from day 16 to 90 (0.17 [0.14–0.24]). Beyond 90 days, the expression level of CD163 did not return to baseline levels (0.11 [0.07–0.13]; *P*<0.0001 with control area as reference; Figure 1B).

We did not find HO-1 positive cells before day 4, when the expression level slightly increased (0.009 [0.005–0.015]). A surge in HO-1 expression was observed from day 8 (0.023 [0.018–0.036]) while the peak of HO-1 expression was observed from 16 to 90 days (0.030 [0.020–0.048]). Beyond 90 days, the expression level of HO-1 almost returned to baseline (0.005 [0.002–0.008]; Figure 1C).

We did not observe iron deposits before day 8, when they significantly appeared and increased gradually over time with a high gap from day 16 (Figure 1D).

On visual examinations, we observed a specific spatial organization of immunolabelled cells. We reported in the Figures 2 through 5 and in Figure S1, the serial neuropathological observations for each immunolabelling and Perl's staining at the 5 different time points.

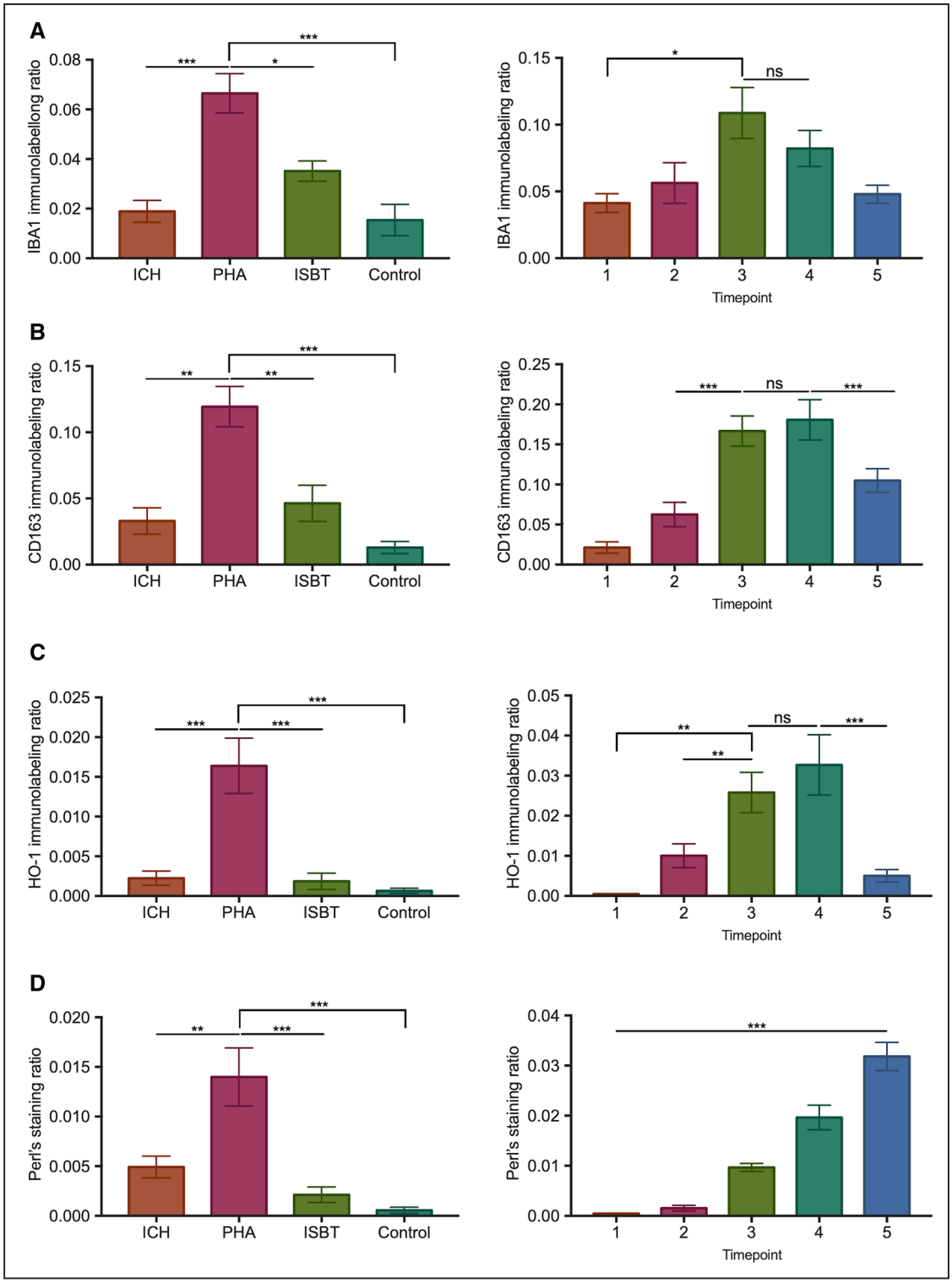

Figure 1. Spatial and temporal distribution of Iba1 (ionized calcium-binding adapter molecule 1), CD163, and HO-1 (hemeoxygenase 1) positive cells and iron deposition.
Immunolabelling ratio ([stacking surface/whole section surface]×10^3) of Iba1 (**A**), CD163 (**B**), HO-1 (**C**), and iron deposition with Perl's staining (**D**) in the brain tissue of 19 patients deceased from spontaneous intracerebral hemorrhage (ICH). On the **left** side, we showed the spatial distribution of markers in the different strategic areas: the hematoma (ICH), the peri-hematomal area (PHA), the ipsilateral surrounding brain tissue (ISBT), and the contralateral control area (control). On the **right** side, we showed the temporal distribution of markers within the PHA at different time periods after onset (T1: ≤72 h, T2: from day 4 to day 7, T3: from day 8 to day 15, T4: from day 16 to day 90 and T5: >day 90). Bars and symbols correspond to the median value and the width of the 95% CI. Ratios were significantly different between time points according to Kruskal-Wallis followed by a Tukey post hoc test (***$P \leq 0.001$, **$P \leq 0.01$, *$P \leq 0.05$). ns indicates not significant.

Gene Expression Profile of Human Perihematomal Tissue

The principal component analysis results did not show any bias towards the conditions or the technique given the clear distinction between both regions of interest PHA and control area (Figure 6A). The number of significantly and differentially expressed genes (under- and over-expressed) with fold change variations >1 for *P*-adjusted <6.10^{-4} was 13/770. HO-1 was the most differentially upregulated gene (2.81±0.39, adjusted $P=1.11\times10^{-10}$). Apart from HO-1, CD163 was the sixth overexpressed gene (1.49±0.29, adjusted $P=1.68\times10^{-5}$). Among the other upregulated genes, we found TNFRSF1b, MMP14, PTX3, IFI30, LAIR1, SERPINE1, SPP1, and SOCS3. Three genes were differentially downregulated: OPALIN, SCL6A1, and GRIN2A (Figure 6B). The detailed statistics of these main results from Nanostring transcriptomic analysis are provided in Table S2. List and results of the 770 genes screened are also available in Table S3.

DISCUSSION

Our study provides novel insights into the natural history of blood clearance after ICH in humans, with a predominant role of CD163/HO-1 pathway.

We first compared the stainings in different strategic areas, and we observed that PHA concentrates most of the activated microglia, recruited monocytes and markers of hemoglobin-scavenging activity. This confirms that PHA is a key area for neuroinflammation and blood clearance after ICH. On visual examination, we observed amoeboid microglia within the PHA, reflecting increased phagocytic activity to clear the brain from toxic components.[22] In a more distant area (ISBT), we observed resting ramified microglia.[23] Basal CD163 expression was extremely low and restricted to perivascular macrophages in contralateral areas. This shows that microglial cells do not express CD163 under physiological conditions, until free hemoglobin is released in the tissue.[24] The abundant perivascular CD163 positive cells within the ISBT suggests that this area is a support for monocyte recruitment.

We then characterized the presence of microglial cells and markers of CD163/HO-1 pathway over time within the PHA.

Interestingly, we observed a specific organization of phagocytic cells with distinct steps: (1) activation of microglia (as early as the first 24 hours), lesion encirclement (from D4), amplification of phagocytosis (with macrophage recruitment, from D8), continuation and then, resorption. Lesion encirclement suggests a cross-talk between microglia and recruited monocytes to limit the spread of neurotoxic compounds arising from hemoglobin degradation. It also appears to be a critical step in blood clearance process given that we did not find

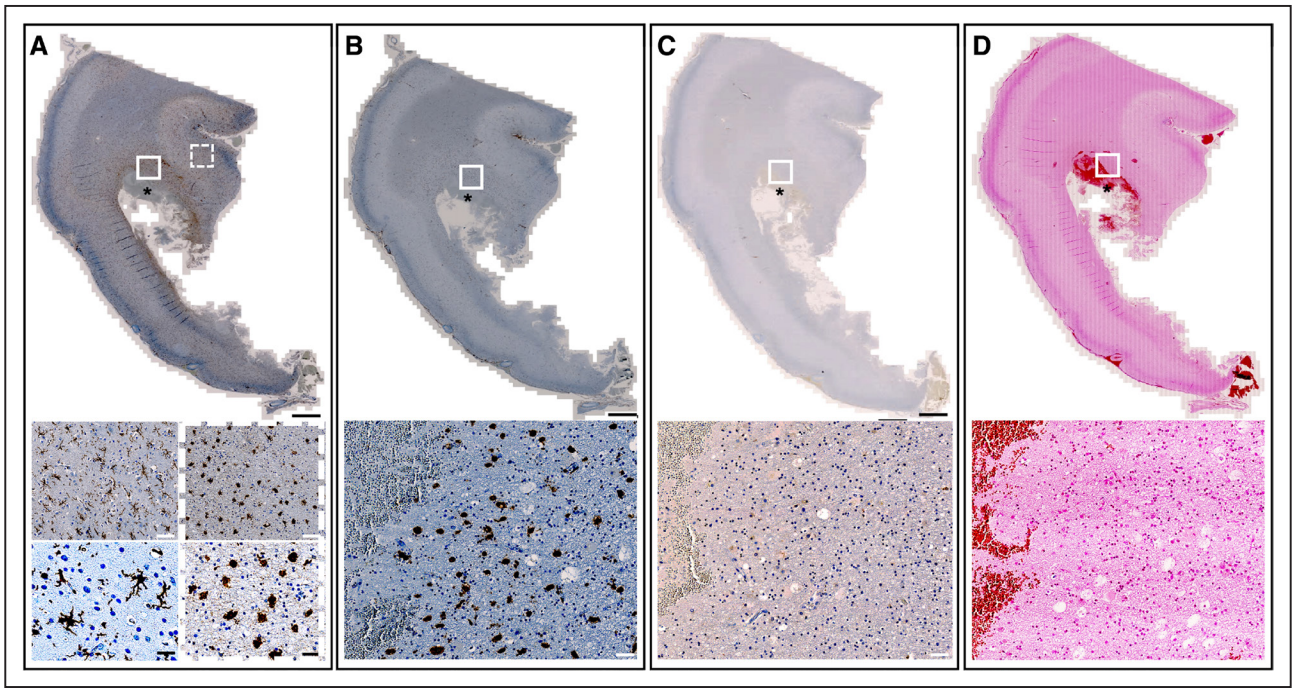

Figure 2. Histopathologic examination of peri-hematomal area (PHA) within 72 hours.
Activation phase Iba1 (ionized calcium-binding adapter molecule 1; **A**), CD163 (**B**), and HO-1 (hemeoxygenase 1; **C**) immunolabellings and Perl's staining (**D**) of adjacent slices of representative peri-hemorrhagic area observed in a patient who deceased 2 days after ICH. Asterisk show the intracerebral hemorrhage (ICH) site. The white squares indicate magnified fields of view under the main block. We observed sparse CD163 positive cells that correspond mainly to resident microglia. We observed numerous ramified (dotted line white square) and ameboid (solid line white square) microglial cells. We did not find any HO-1 positive cell nor iron deposit. Scale bars=2 cm for main bloc, 50 µm for upper magnified fields of view and 20 µm for bottom magnified fields of view.

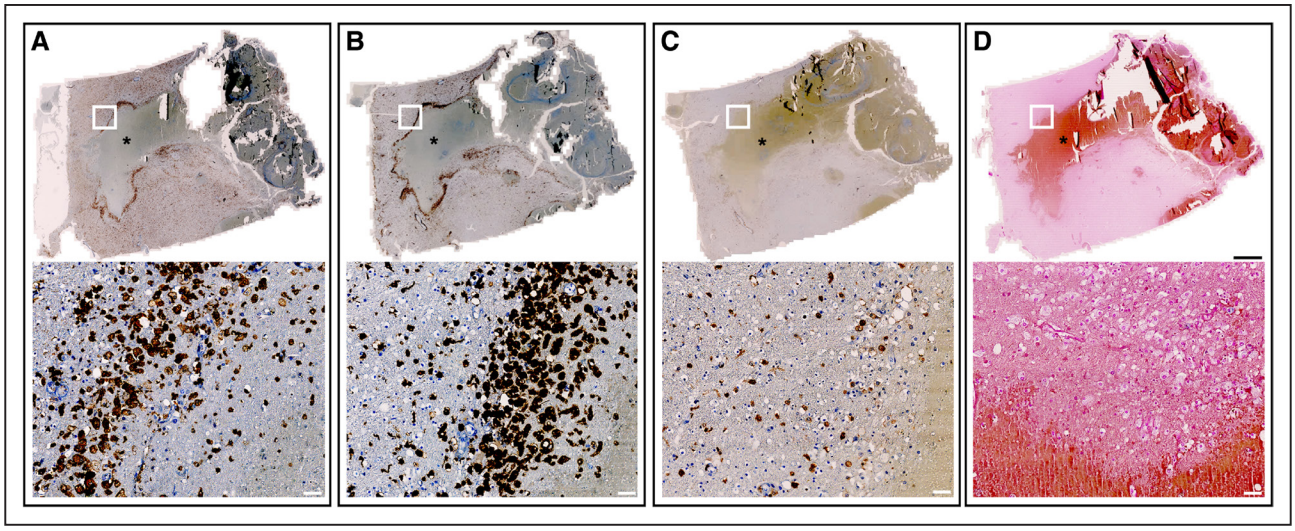

Figure 3. Histopathologic examination of peri-hematomal area (PHA) from day 4 to day 7: encircling and induction phase. Iba1 (ionized calcium-binding adapter molecule 1; **A**), CD163 (**B**), and HO-1 (hemeoxygenase 1; **C**) immunolabellings and Perl's staining (**D**) of adjacent slices of representative peri-hemorrhagic area observed in a patient who deceased 5 days after intracerebral hemorrhage (ICH). Asterisk show the ICH site. The white squares indicate magnified fields of view under the main block. We noted a specific spatial organization of microglia and monocytes that became more abundant and encircled the ICH core. HO-1 was sparsely observed, but no iron deposit was detected. Scale bars=2 cm for main bloc, 50 μm for magnified fields of view.

any HO-1 positive cell before this circle formation. The D8-D15 time window was critical for blood clearance process amplification. The HO-1 marker became, therefore, much more abundant and was accompanied by a progressive iron accumulation, suggesting the generation of siderophages. Our findings regarding iron deposits differ from the kinetics of events described in animal models. Indeed in animal models, iron deposits peak between 3 and 7 days,[25] whereas in our study, iron deposits were not observed until day 8. This suggests that the blood clearance process might be effective earlier in animals than in humans. It also highlights the difficult translation of data observed in healthy young animals to elderly patients with comorbidities. Of note, Iba1 and CD163 expression levels remained high several months to years after ICH, suggesting a chronic proinflammatory status that might be harmful for the brain tissue.

Since we observed a strategic time-window in the blood clearance process, we proceeded to RNA extraction from PHA in patients who deceased around D8 to

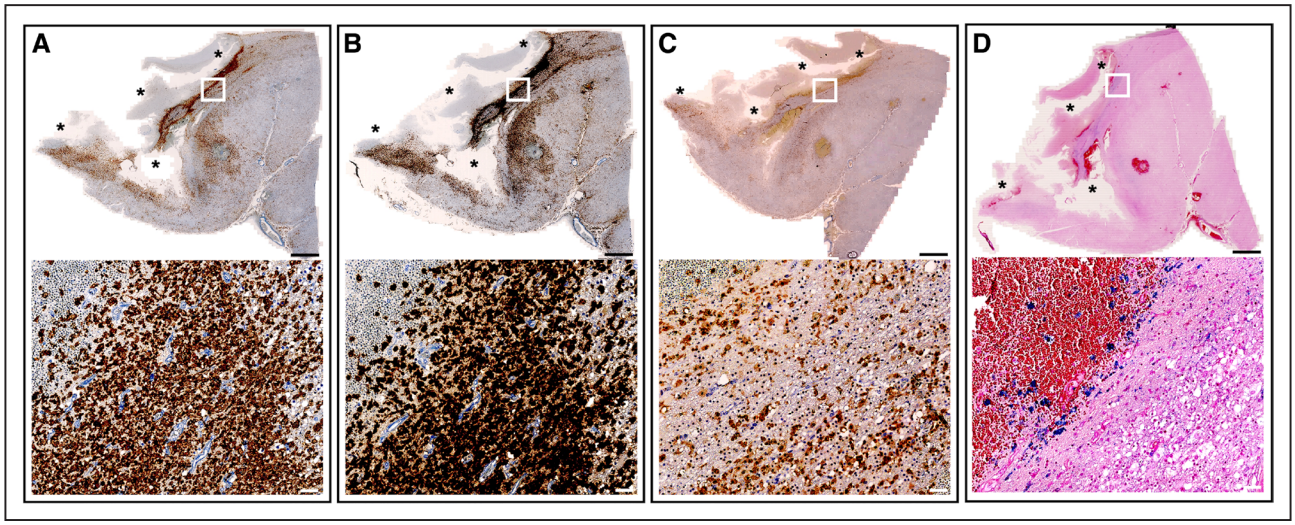

Figure 4. Histopathologic examination of peri-hematomal area (PHA) from day 8 to day 15: amplification phase. Iba1 (ionized calcium-binding adapter molecule 1; **A**), CD163 (**B**), and HO-1 (hemeoxygenase 1; **C**) immunolabellings and Perl's staining (**D**) of adjacent slices of representative peri-hemorrhagic area observed in a patient who deceased 13 days after intracerebral hemorrhage (ICH). Asterisks show the ICH site. The white squares indicate magnified fields of view under the main block. We observed an abundant amount of ameboid microglia and CD163 positive cells surrounding the hematoma core. HO-1 positive cells were also more abundant and first iron deposits appeared (blue). All these substantial changes indicated an amplification of the blood clearance process. Scale bars=2 cm for main bloc, 50 μm for magnified fields of view.

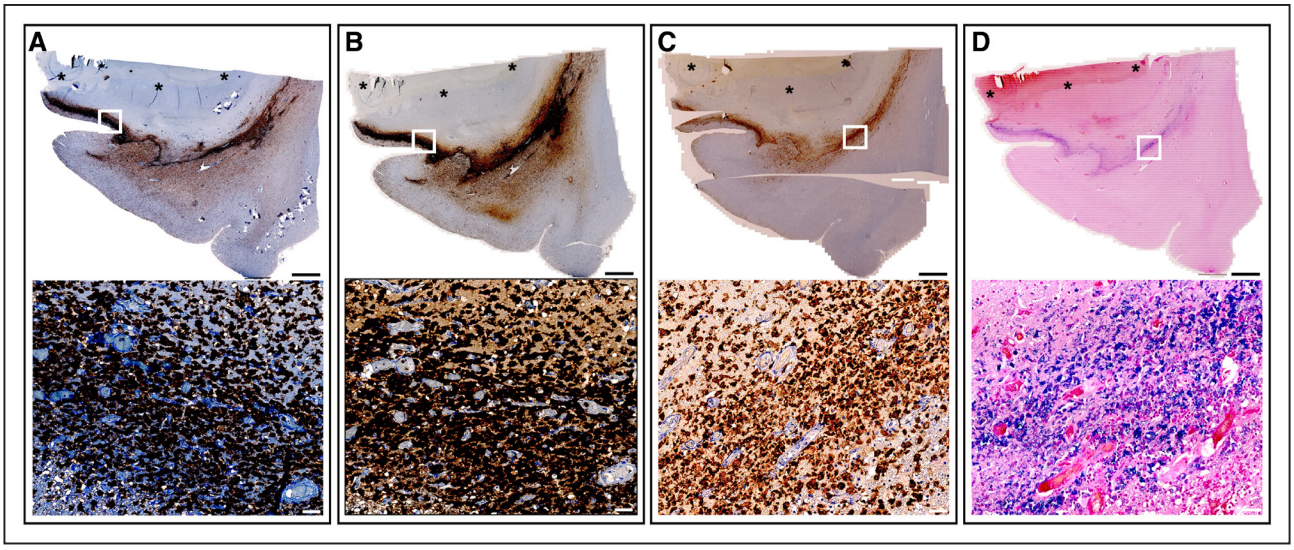

Figure 5. Histopathologic examination of peri-hematomal area (PHA) from day 16 to day 90: continuation phase. Iba1 (ionized calcium-binding adapter molecule 1; **A**), CD163 (**B**), and HO-1 (hemeoxygenase 1; **C**) immunolabellings and Perl's staining (**D**) of adjacent slices of representative peri-hemorrhagic area observed in a patient who deceased 30 days after intracerebral hemorrhage (ICH). Asterisks show the ICH site. The white squares indicate magnified fields of view under the main block. We noted an increase in microglia/monocyte cells signal that still encircled the lesion. HO-1 activity was also increased and fitted with iron accumulation (blue). Scale bars=2 cm for main bloc, 50 µm for magnified fields of view.

D15. This transcriptomic analysis confirmed the predominant expression of CD163/HO-1 pathway. To our knowledge, only 4 studies investigated specifically CD163 and HO-1 expression after ICH in human neuropathological samples. Most of them were based on per-operative biopsies and focused on early phase of the disease (<72 hours after ICH onset).[15–18] In our study, we also observed CD163 and HO-1 from 24 and 72 hours, respectively, but their expressions became much more abundant from day 8.

The evidence for CD163/HO-1 involvement in ICH human tissue justifies experimental research efforts targeting this pathway. Treatments that enhance the phagocytic function of microglia/macrophages may be promising to reduce the toxicity of blood products. It is also noteworthy that soluble CD163 can be monitored in the plasma of patients to predict their clinical and radiological outcome after ICH.[26] One can hypothesize a future personal based medicine to identify which patients with ICH are exposed to CD163/HO-1 overwhelming and may benefit from pharmacomodulation.

Beyond the genomic evidence for CD163/HO-1 overexpression, our transcriptomic analysis provided valuable information on peri-hematomal tissue changes. PHA has been reported to suffer from edema, apoptosis, necrosis, and inflammatory processes, enhancing the so-called secondary tissue injuries. However, we also identified several upregulated genes that exert a beneficial role in terminating inflammation and enhancing tissue repair. TNFRSF1b (tumor necrosis factor receptor superfamily member 1B, also known as TNFR2) might regulate inflammation by promoting the expression of anti-inflammatory genes in microglia,[27] protect neurons by preventing apoptosis through antioxidative pathways[28] and repair the ICH-damaged tissue by contributing to remyelination.[29] Other genes play an important role in macrophage and microglial cell polarization by repressing the M1 proinflammatory phenotype: The LAIR1 gene encoding the leukocyte-associated immunoglobulin-like receptor 1 protein, SOCS3, a member of the suppressor of cytokine signaling family and the PTX3 (long pentraxin 3), a member of the pentraxin superfamily of prototypic humoral pattern recognition molecules. These genes coordinate the transition from an acute inflammatory phase to a phagocytic phase promoting hematoma resolution or tissue repair.[30–32] Among these 3 genes, PTX3 is of particular interest. Its upregulation is induced by thrombin supporting a role in ICH.[33] It also contributes to tissue remodeling and repair, through an interaction with fibrinogen/fibrin, collagen and plasminogen, a group of proteins present in the PHA.[34,35] The MMP-14 (membrane-type 1 matrix metalloproteinase-14), known as expressed by microglia and recruited macrophages, can also act as a negative regulator of inflammation.[36] The IFI30 gene encodes the GILT (gamma-interferon-inducible lysosomal thiol reductase) enzyme and plays an important role in antigen processing by enhancing the major histocompatibility complex class II-restricted presentation.[37] The secreted phosphoprotein 1 (Spp1) gene encodes the osteopontin (OPN) protein. *OPN* acts as an immune modulator, regulating the expression of interferon-gamma and interleukin-1, and promotes cell survival by inhibiting apoptosis.[38] Over-expression these genes suggest that a transition to an anti-inflammatory phase within the PHA provides a suitable microenvironment for the acquisition of hemoglobin-scavenger

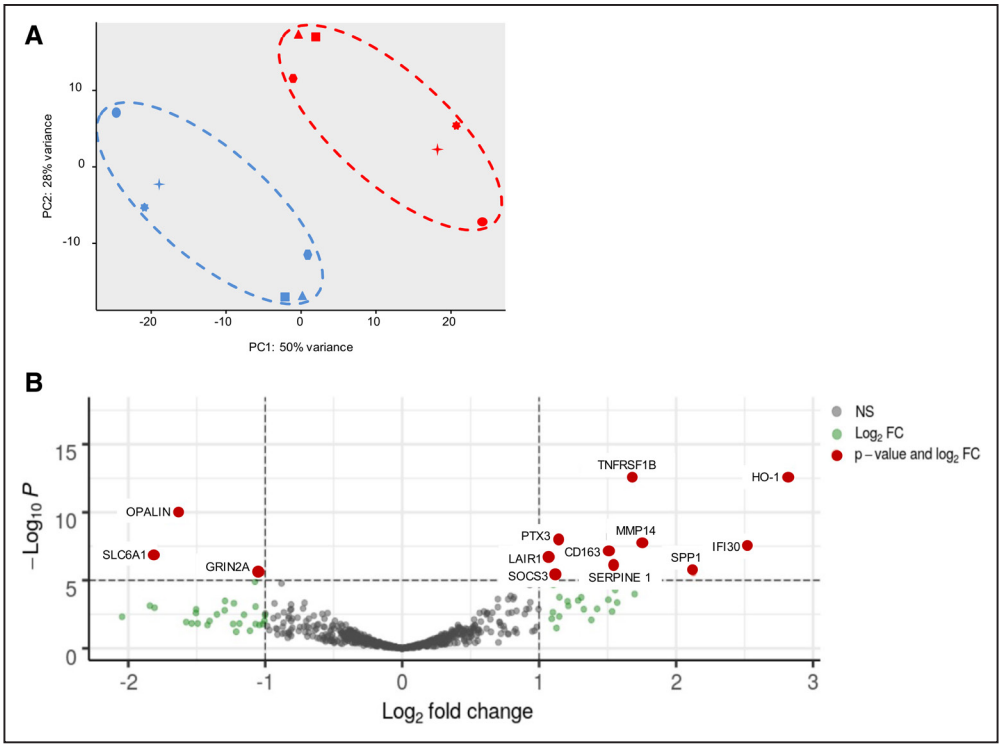

Figure 6. Genomic study of peri-hematomal area (PHA).
Data provided from 6 patients who deceased from day 6 to day 15 after intracerebral hemorrhage (ICH). We compared PHA to a contralateral area as a reference. **A**, Principal component analysis based on Variance Stabilizing transformation of molecule counts: each symbol corresponds to one patient. Localization is highlighted by a color (red=PHA, blue=control area). **B**, Volcano-plot: Scatter plot of the significance of expression of all genes in perihematomal tissue *vs* control. *y* axis is *P* value at log-scale obtained with DEseq2 package. *x* axis is the gene expression log fold change of PHA vs control. Red dots are genes that are significantly expressed in PHA vs control area and having an absolute value of log2 fold change above or equal 1. Green dots are genes that are not significantly expressed in perihematomal vs control, but with an absolute log2 fold change below 1 between both groups.

properties by microglia and macrophages. This is an important information for potential therapeutic strategies targeting neuroinflammation that should ensure this transition from a proinflammatory to an anti-inflammatory status.

In line with previous work,[39] we found an upregulation of SERPINE 1 (serpin family E member 1) that may have a deleterious effect in an ICH setting. This gene encodes a member of the serine protease inhibitor superfamily, the principal inhibitor of tissue-type plasminogen activator (PAI-1). In addition to its role in the regulation of fibrinolysis, PAI-1 is thought to be a proinflammatory mediator.[40] Since triggered by hem accumulation, SERPINE1 might precipitate hem-induced neuronal apoptosis and inflammation in an ICH setting.[41]

Three downregulated genes indicated tissular injury. We found a decrease in expression levels of key genes of myelin assembly such as OPALIN (oligodendrocyte myelin paranodal and inner loop protein), a marker of mature oligodendrocytes.[42] The downregulation of SLC6A1 (solute carrier family 6 member 1) (encoding GAT-1 [γ-aminobutyric acid transporter 1], one of the major γ-aminobutyric acid transporters in the brain) and GRIN2A (gutamate ionotropic receptor NMDA type subunit 2A; (encoding the *N*-methyl-D-aspartate receptor subunit GluN2A) suggests a disturbance in cerebral neurotransmission following ICH.[43] In addition to its role in neurotransmission and neuronal development, γ-aminobutyric acid also modulates inflammation and has an inhibitory role in the immune system (decrease of inflammatory cytokine production).[44]

According to a recent meta-analysis, only 2 studies (one postmortem and one on per-operative biopsies) used transcriptomic methods to assess gene expression within the PHA.[45] Rosell et al[39] reported transcriptomic analysis from 4 cases who died within 4 days after ICH. Interestingly, CD163 expression was among the most differentially upregulated molecules but authors did not report results on HO-1 expression. Carmichael et al[46] did not find any upregulation of HO-1 and did not mention CD163. However, their 6 samples were obtained within the first 24 hours after ICH while we mostly observed HO-1 positive cells from day 8.

Our study has some limitations. We acknowledge that the cross-sectional nature of our post-mortem study and the small sample size within each time interval prevented us from further evaluating dynamic changes over time. We focused our transcriptomic analysis on selected cases who died around the D7-D15 time-window when

we observed significant changes in histological examinations, possibly leading to selection bias. Further study will aim at investigating changes of transcriptomic expression across different time intervals. In addition, we cannot exclude that the consent for brain banking introduce a potential bias that may affect generalizability of our results. Our study population included elderly patients, and ICH was associated with underlying cerebral amyloid angiopathy in 18/19 cases. Therefore, age and type of underlying vessel disease may have contributed to our findings. However, the patient with a deep ICH showed similar histological features as lobar ICH cases at similar timepoints. Of note, except for one patient (deceased 8 months after ICH), no significant neuroinflammation was found in the contralateral hemispheres, suggesting that the changes observed in this latter case were related to the bleeding event and not to the nature of the underlying vasculopathy. Once recruited monocytes differentiate into brain macrophages, they are nearly indistinguishable from reactive microglia and they both express CD163. Therefore, we cannot differentiate the contribution of resident microglia from infiltrating macrophages.

Our study has also strengths. Despite the cross-sectional nature of a histopathologic study, we obtained several samples at different timepoints that appeared relevant in the natural history of severe ICH. We combined neuropathological and genomic explorations to investigate blood clearance mechanisms. We used an immunohistochemistry automated staining machine and semi-automated technique to quantify immunolabelling of the sections, ensuring reproducibility of our results.

In conclusion, we provide histological and genomic-based evidence in humans for the predominant expression of CD163/HO-1 pathway in the PHA, with a strategic time-window: from day 8 to 15 after ICH. An anti-inflammatory environment seems suitable for the enhancement of the endogenous blood clearance process. Our findings contribute to identify innovative therapeutic strategies for ICH.

ARTICLE INFORMATION

Received October 19, 2021; final revision received March 1, 2022; accepted March 22, 2022.

Affiliations

Univ. Lille, Inserm, CHU-Lille, Lille Neuroscience & Cognition research Center UMR-S1172, Degenerative and Vascular Cognitive Disorders, France (L.P., R.P., V.D., C.C., V.B.). Alzheimer Research Unit, Department of Neurology, Massachusetts General Hospital, Charlestown (R.P.). Harvard Medical School, Boston, MA (R.P.). Univ. Lille, CNRS, Inserm, CHU Lille, Institut Pasteur de Lille, US 41 - UMS 2014 - PLBS, France (M.F.). Univ. Lille, CNRS, Inserm, CHU Lille, UMR9020-U1277 - CANTHER - Cancer Heterogeneity Plasticity and Resistance to Therapies, Lille, France (B.D.). Université d'Artois, Lens, France (V.B.).

Acknowledgments

We thank Marie-Hélène Gevaert, (Department of Histology, Lille) for her technical assistance in immunolabelling. We thank Pr Isabelle Van Seuningen for access to the immunohistochemistry platform of the Canther laboratory (UMR9020 CNRS-U1277 Inserm). We thank Shéhérazade Sebda from the GO@L-GFS, Plateformes Lilloises en Biologie et Santé (PLBS)—UMS 2014—US 41 for Nanostring experimentations. Drs Puy, Bérézowski, and Cordonnier contributed to the conception of the study, drafted the article; Dr Puy, Dr Bérézowski, B. Duchêne, Dr Perbet, Dr Figeac, and Dr Deramecourt contributed to the acquisition and analysis of the data.

Sources of Funding

This work was supported by the Fondation Recherche sur les Accidents Vasculaires Cérébraux (project FRAVC180713012), the Fondation pour la Recherche Médicale (FDM201806006375, fellowship Dr Puy) and the Fondation I-SITE ULNE (fellowship Dr Puy).

Disclosures

None.

Supplemental Material

Tables S1–S3
Figure S1

REFERENCES

1. van Asch CJ, Luitse MJ, Rinkel GJ, van der Tweel I, Algra A, Klijn CJ. Incidence, case fatality, and functional outcome of intracerebral haemorrhage over time, according to age, sex, and ethnic origin: a systematic review and meta-analysis. *Lancet Neurol.* 2010;9:167–176. doi: 10.1016/S1474-4422(09)70340-0
2. Aronowski J, Zhao X. Molecular pathophysiology of cerebral hemorrhage: secondary brain injury. *Stroke.* 2011;42:1781–1786. doi: 10.1161/STROKEAHA.110.596718
3. Hanley DF, Thompson RE, Rosenblum M, Yenokyan G, Lane K, McBee N, Mayo SW, Bistran-Hall AJ, Gandhi D, Mould WA, et al; MISTIE III Investigators. Efficacy and safety of minimally invasive surgery with thrombolysis in intracerebral haemorrhage evacuation (MISTIE III): a randomised, controlled, open-label, blinded endpoint phase 3 trial. *Lancet.* 2019;393:1021–1032. doi: 10.1016/S0140-6736(19)30195-3
4. Jing C, Bian L, Wang M, Keep RF, Xi G, Hua Y. Enhancement of hematoma clearance with CD47 blocking antibody in experimental intracerebral hemorrhage. *Stroke.* 2019;50:1539–1547. doi: 10.1161/STROKEAHA.118.024578
5. Chen-Roetling J, Lu X, Regan RF. Targeting heme oxygenase after intracerebral hemorrhage. *Ther Targets Neurol Dis.* 2015;2:474. doi: 10.14800/ttnd.474
6. Graversen JH, Moestrup SK. Drug trafficking into macrophages via the endocytotic receptor CD163. *Membranes (Basel).* 2015;5:228–252. doi: 10.3390/membranes5020228
7. Kristiansen M, Graversen JH, Jacobsen C, Sonne O, Hoffman HJ, Law SK, Moestrup SK. Identification of the haemoglobin scavenger receptor. *Nature.* 2001;409:198–201. doi: 10.1038/35051594
8. Schaer DJ, Buehler PW, Alayash AI, Belcher JD, Vercellotti GM. Hemolysis and free hemoglobin revisited: exploring hemoglobin and hemin scavengers as a novel class of therapeutic proteins. *Blood.* 2013;121:1276–1284. doi: 10.1182/blood-2012-11-451229
9. Dixon SJ, Stockwell BR. The role of iron and reactive oxygen species in cell death. *Nat Chem Biol.* 2014;10:9–17. doi: 10.1038/nchembio.1416
10. Campbell NK, Fitzgerald HK, Dunne A. Regulation of inflammation by the antioxidant haem oxygenase 1. *Nat Rev Immunol.* 2021;21:411–425. doi: 10.1038/s41577-020-00491-x
11. Thomsen JH, Etzerodt A, Svendsen P, Moestrup SK. The haptoglobin-CD163-heme oxygenase-1 pathway for hemoglobin scavenging. *Oxid Med Cell Longev.* 2013;2013:523652. doi: 10.1155/2013/523652
12. Leclerc JL, Lampert AS, Loyola Amador C, Schlakman B, Vasilopoulos T, Svendsen P, Moestrup SK, Doré S. The absence of the CD163 receptor has distinct temporal influences on intracerebral hemorrhage outcomes. *J Cereb Blood Flow Metab.* 2018;38:262–273. doi: 10.1177/0271678X17701459
13. Liu R, Cao S, Hua Y, Keep RF, Huang Y, Xi G. CD163 expression in neurons after experimental intracerebral hemorrhage. *Stroke.* 2017;48:1369–1375. doi: 10.1161/STROKEAHA.117.016850
14. Garton T, Keep RF, Hua Y, Xi G. CD163, a hemoglobin/haptoglobin scavenger receptor, after intracerebral hemorrhage: functions in microglia/macrophages versus neurons. *Transl Stroke Res.* 2017;8:612–616. doi: 10.1007/s12975-017-0535-5

15. Zhang XW, Wu Y, Wang DK, Jin X, Li CH. Expression changes of inflammatory cytokines TNF-α, IL-1β and HO-1 in hematoma surrounding brain areas after intracerebral hemorrhage. *J Biol Regul Homeost Agents*. 2019;33:1359–1367. doi: 10.23812/19-150-A
16. Liu B, Hu B, Shao S, Wu W, Fan L, Bai G, Shang P, Wang X. CD163/Hemoglobin Oxygenase-1 pathway regulates inflammation in hematoma surrounding tissues after intracerebral hemorrhage. *J Stroke Cerebrovasc Dis*. 2015;24:2800–2809. doi: 10.1016/j.jstrokecerebrovasdis.2015.08.013
17. Duan SR, Wang XR, Wang CY, Wang DS, Qi JP, Wang HT. [Expressions of heme oxygenase-1 and apoptosis-modulating proteins in peri-hematoma cortex after intracerebral hemorrhage in human being]. *Zhonghua Yi Xue Za Zhi*. 2007;87:1904–1907.
18. Holfelder K, Schittenhelm J, Trautmann K, Haybaeck J, Meyermann R, Beschorner R. De novo expression of the hemoglobin scavenger receptor CD163 by activated microglia is not associated with hemorrhages in human brain lesions. *Histol Histopathol*. 2011;26:1007–1017. doi: 10.14670/HH-26.1007
19. Deramecourt V, Slade JY, Oakley AE, Perry RH, Ince PG, Maurage CA, Kalaria RN. Staging and natural history of cerebrovascular pathology in dementia. *Neurology*. 2012;78:1043–1050. doi: 10.1212/WNL.0b013e31824e8e7f
20. Puy L, Corseaux D, Perbet R, Deramecourt V, Cordonnier C, Bérézowski V. Neutrophil extracellular traps (NETs) infiltrate haematoma and surrounding brain tissue after intracerebral haemorrhage: A post-mortem study. *Neuropathol Appl Neurobiol*. 2021;47:867–877. doi: 10.1111/nan.12733
21. Love MI, Huber W, Anders S. Moderated estimation of fold change and dispersion for RNA-seq data with DESeq2. *Genome Biol*. 2014;15:550. doi: 10.1186/s13059-014-0550-8
22. Shtaya A, Bridges LR, Esiri MM, Lam-Wong J, Nicoll JAR, Boche D, Hainsworth AH. Rapid neuroinflammatory changes in human acute intracerebral hemorrhage. *Ann Clin Transl Neurol*. 2019;6:1465–1479. doi: 10.1002/acn3.50842
23. Davis BM, Salinas-Navarro M, Cordeiro MF, Moons L, De Groef L. Characterizing microglia activation: a spatial statistics approach to maximize information extraction. *Sci Rep*. 2017;7:1576. doi: 10.1038/s41598-017-01747-8
24. Xue M, Del Bigio MR. Intracerebral injection of autologous whole blood in rats: time course of inflammation and cell death. *Neurosci Lett*. 2000;283:230–232. doi: 10.1016/s0304-3940(00)00971-x
25. Xiong XY, Wang J, Qian ZM, Yang QW. Iron and intracerebral hemorrhage: from mechanism to translation. *Transl Stroke Res*. 2014;5:429–441. doi: 10.1007/s12975-013-0317-7
26. Roy-O'Reilly M, Zhu L, Atadja L, Torres G, Aronowski J, McCullough L, Edwards NJ. Soluble CD163 in intracerebral hemorrhage: biomarker for perihematomal edema. *Ann Clin Transl Neurol*. 2017;4:793–800. doi: 10.1002/acn3.485
27. Veroni C, Gabriele L, Canini I, Castiello L, Coccia E, Remoli ME, Columba-Cabezas S, Aricò E, Aloisi F, Agresti C. Activation of TNF receptor 2 in microglia promotes induction of anti-inflammatory pathways. *Mol Cell Neurosci*. 2010;45:234–244. doi: 10.1016/j.mcn.2010.06.014
28. Probert L. TNF and its receptors in the CNS: the essential, the desirable and the deleterious effects. *Neuroscience*. 2015;302:2–22. doi: 10.1016/j.neuroscience.2015.06.038
29. Patel JR, Williams JL, Muccigrosso MM, Liu L, Sun T, Rubin JB, Klein RS. Astrocyte TNFR2 is required for CXCL12-mediated regulation of oligodendrocyte progenitor proliferation and differentiation within the adult CNS. *Acta Neuropathol*. 2012;124:847–860. doi: 10.1007/s00401-012-1034-0
30. Qin H, Holdbrooks AT, Liu Y, Reynolds SL, Yanagisawa LL, Benveniste EN. SOCS3 deficiency promotes M1 macrophage polarization and inflammation. *J Immunol*. 2012;189:3439–3448. doi: 10.4049/jimmunol.1201168
31. Carvalheiro T, Garcia S, Pascoal Ramos MI, Giovannone B, Radstake TRDJ, Marut W, Meyaard L. Leukocyte associated immunoglobulin like receptor 1 regulation and function on monocytes and dendritic cells during inflammation. *Front Immunol*. 2020;11:1793. doi: 10.3389/fimmu.2020.01793
32. Jin J, Wang Y, Ma Q, Wang N, Guo W, Jin B, Fang L, Chen L. LAIR-1 activation inhibits inflammatory macrophage phenotype in vitro. *Cell Immunol*. 2018;331:78–84. doi: 10.1016/j.cellimm.2018.05.011
33. López ML, Bruges G, Crespo G, Salazar V, Deglesne PA, Schneider H, Cabrera-Fuentes H, Schmitz ML, Preissner KT. Thrombin selectively induces transcription of genes in human monocytes involved in inflammation and wound healing. *Thromb Haemost*. 2014;112:992–1001. doi: 10.1160/TH14-01-0034
34. Shiraki A, Kotooka N, Komoda H, Hirase T, Oyama JI, Node K. Pentraxin-3 regulates the inflammatory activity of macrophages. *Biochem Biophys Rep*. 2016;5:290–295. doi: 10.1016/j.bbrep.2016.01.009
35. Doni A, Stravalaci M, Inforzato A, Magrini E, Mantovani A, Garlanda C, Bottazzi B. The Long Pentraxin PTX3 as a link between innate immunity, tissue remodeling, and cancer. *Front Immunol*. 2019;10:712. doi: 10.3389/fimmu.2019.00712
36. Fingleton B. Matrix metalloproteinases as regulators of inflammatory processes. *Biochim Biophys Acta Mol Cell Res*. 2017;1864(11 pt A):2036–2042. doi: 10.1016/j.bbamcr.2017.05.010
37. Satoh JI, Kino Y, Yanaizu M, Ishida T, Saito Y. Microglia express gamma-interferon-inducible lysosomal thiol reductase in the brains of Alzheimer's disease and Nasu-Hakola disease. *Intractable Rare Dis Res*. 2018;7:251–257. doi: 10.5582/irdr.2018.01119
38. Rittling SR, Singh R. Osteopontin in immune-mediated diseases. *J Dent Res*. 2015;94:1638–1645. doi: 10.1177/0022034515605270
39. Rosell A, Vilalta A, García-Berrocoso T, Fernández-Cadenas I, Domingues-Montanari S, Cuadrado E, Delgado P, Ribó M, Martínez-Sáez E, Ortega-Aznar A, et al. Brain perihematoma genomic profile following spontaneous human intracerebral hemorrhage. *PLoS One*. 2011;6:e16750. doi: 10.1371/journal.pone.0016750
40. Sillen M, Declerck PJ. A narrative review on Plasminogen Activator Inhibitor-1 and its (Patho)physiological role: to target or not to target? *Int J Mol Sci*. 2021;22:2721. doi: 10.3390/ijms22052721
41. Wang T, Lu H, Li D, Huang W. TGF-β1-mediated activation of SERPINE1 is involved in hemin-induced apoptotic and inflammatory injury in HT22 cells. *Neuropsychiatr Dis Treat*. 2021;17:423–433. doi: 10.2147/NDT.S293772
42. Kippert A, Trajkovic K, Fitzner D, Opitz L, Simons M. Identification of Tmem10/Opalin as a novel marker for oligodendrocytes using gene expression profiling. *BMC Neurosci*. 2008;9:40. doi: 10.1186/1471-2202-9-40
43. Strehlow V, Heyne HO, Vlaskamp DRM, Marwick KFM, Rudolf G, de Bellescize J, Biskup S, Brilstra EH, Brouwer OF, Callenbach PMC, et al; GRIN2A study group. GRIN2A-related disorders: genotype and functional consequence predict phenotype. *Brain*. 2019;142:80–92. doi: 10.1093/brain/awy304
44. Bhat R, Axtell R, Mitra A, Miranda M, Lock C, Tsien RW, Steinman L. Inhibitory role for GABA in autoimmune inflammation. *Proc Natl Acad Sci USA*. 2010;107:2580–2585. doi: 10.1073/pnas.0915139107
45. Loan JJ, Kirby C, Emelianova K, Dando OR, Poon MT, Pimenova L, Hardingham GE, McColl BW, Klijn CJ, Al-Shahi Salman R, et al. Secondary injury and inflammation after intracerebral haemorrhage: a systematic review and meta-analysis of molecular markers in patient brain tissue. *J Neurol Neurosurg Psychiatry*. 2022;93:126–132. doi: 10.1136/jnnp-2021-327098
46. Carmichael ST, Vespa PM, Saver JL, Coppola G, Geschwind DH, Starkman S, Miller CM, Kidwell CS, Liebeskind DS, Martin NA. Genomic profiles of damage and protection in human intracerebral hemorrhage. *J Cereb Blood Flow Metab*. 2008;28:1860–1875. doi: 10.1038/jcbfm.2008.77